Permeability and effective porosity of porous media

A. Koponen, M. Kataja, and J. Timonen
Department of Physics, University of Jyväskylä, P.O. Box 35, FIN-40351 Jyväskylä, Finland
(Received 4 December 1996)

The concept of permeability of porous media is discussed, and a modification of Kozeny's permeability equation to include the effect of effective porosity is introduced. An analytical expression for the specific surface area of a system constructed of randomly placed identical obstacles with unrestricted overlap is derived, and a lattice-gas cellular automaton method is then used to simulate the dependence on porosity of permeability, tortuosity, and effective porosity for a flow of Newtonian uncompressible fluid in this two-dimensional porous substance. The simulated permeabilities can well be explained by the concept of effective porosity, and the exact form of the specific surface area. The critical exponent of the permeability near the percolation threshold is also determined from the simulations. [S1063-651X(97)11109-6]

PACS number(s): 47.55.Mh, 47.15.−x

I. INTRODUCTION

Studies of flow through porous media have mainly been concerned with the derivation of macroscopic laws for the fluid flow. For the case of creeping flow of a single viscous fluid through a porous medium, e.g., the phenomenological law first discovered by Darcy,

$$\mathbf{q} = -\frac{k}{\mu}\nabla p, \tag{1}$$

is known to hold for a wide variety of natural porous media ranging from loose sand to tight granite rocks [1–3]. Here $\mathbf{q}$ is the flux of the fluid through the porous medium, μ is the viscosity of the fluid, and p is the fluid pressure. The permeability coefficient k is a measure of fluid conductivity through the substance.

The prediction of the permeability k in Eq. (1) for various porous media has been a long-standing problem of great practical relevance. The experimental methods used in the studies have varied from rather straightforward measurements [3–6] to more sophisticated approaches, which utilize, e.g., mercury porosimetry, electrical conductivity, nuclear magnetic resonance, and acoustic properties of the medium [6–12]. Theoretical work has often involved models with simplified pore geometries, which allows an analytical solution of the microscopic flow patterns [1,2,13]. More sophisticated models based on statistical methods have also been used [2,3,14]. However, due to the extremely complex nature of the phenomena involved, many basic questions remain unanswered. Various correlations between the permeability and the parameters describing the geometrical properties of the medium have been suggested, but a general form for the permeability as a function of porosity is still lacking.

Percolation theory is an invaluable tool in the theoretical studies of flow phenomena in porous media and fractured rock [15,16]. Percolation concepts are also essential for the correct interpretation of many experimental data. The study of percolation properties of fluid flow in a porous medium is usually very difficult. In this work we use direct numerical simulations to find the scaling law for the permeability of a two-dimensional porous medium.

During the last few years, rapid development of computers and computational algorithms has made possible direct simulations of complicated fluid flow phenomena. Among the promising new methods are lattice-gas and lattice Boltzmann methods [17–23] that can be applied to a large variety of fluid flow problems. The geometrical versatility of these methods makes them particularly useful in simulating flows in irregular geometries [24–34].

In this paper we use the lattice-gas method to simulate numerically a creeping flow of Newtonian fluid through a two-dimensional porous substance that consists of randomly placed rectangles of equal size and unrestricted overlap. Within this numerical approach, we study correlations between various macroscopic parameters such as permeability, porosity, effective porosity, specific surface area and tortuosity, which are often used to characterize transport phenomena in porous media. The model of porous medium used in this work is chosen mainly because it is possible to derive in this case an exact expression for the specific surface area. This is useful when comparing simulation results with theoretically derived expressions. To this end the concept of effective porosity was found to be of crucial importance, in explaining the simulated permeability in particular. The behavior of permeability near the percolation threshold was also analyzed.

II. PERMEABILITY OF A POROUS SUBSTANCE

In theoretical and experimental work on fluid flow in porous media it is typically attempted to find functional correlations between the permeability and some other macroscopic properties of the porous medium. Among the most important of such properties are the porosity ϕ and the specific surface area S, which give the ratios of the total void volume and the total interstitial surface area to the bulk volume, respectively. Another useful characteristic of porous media is the tortuosity τ, which has been introduced to account for the complexity of the actual microscopic flow paths through the substance. Tortuosity can be defined as the ratio of a (properly weighted) average length of microscopic flow paths to the length of the system in the direction of the macroscopic flux [35].

Simple dimensional analysis suggests that the permeability of a porous medium is of the form $k=f(\phi,\tau)/S^2$, where $f(\phi,\tau)$ is a dimensionless function of ϕ and τ. Various simplified models can be used to find suitable candidates for f. Darcy's law, Eq. (1), can easily be derived within the simple capillary theory by Kozeny, in which the porous medium is envisaged as a layer of solid material with straight parallel tubes of a fixed cross-sectional shape intersecting the sample. Within this model, the permeability is explicitly given as

$$k=\frac{\phi^3}{cS^2}, \tag{2}$$

where c is the Kozeny coefficient that depends on the cross section of the capillaries. For cylindrical capillaries, $c=2$. The simplest way to introduce tortuosity in the capillary model is to allow the tubes to be inclined in such a way that the axes of the capillaries form a fixed angle θ with the normal of the surface of the material (while the azimuthal angle of the tubes is randomly distributed). In this case the permeability becomes

$$k=\frac{\phi^3}{c\tau^2S^2}, \tag{3}$$

where $\tau=1/\cos\theta$ is the tortuosity of the medium. Equations (2) and (3) are perhaps the most widely used expressions for the permeability of a porous medium. Porous media can often be found to conform to them, although quantitative agreement should not generally be expected. For systems composed of randomly placed obstacles, e.g., permeability behaves for high porosities ($\phi\to1$) as $1/(1-\phi)$, and the Kozeny model is not valid.

While considering flow through a porous medium, only the interconnected pores are of interest, as the occluded pores (pores not connected to the main void space) do not contribute to the flow. (The term porosity is sometimes used to include the interconnected pore space only.) The dead-end pores are another type of pores that contribute very little to the flow. These pores belong to the interconnected pores, but, owing to their geometry, no global pathlines intersect them. The occluded pores and the dead-end pores form the nonconducting pore space of the medium. The effective porosity $\phi_{\rm eff}$ of a porous medium can be defined as the ratio of the volume of the conducting pores to the total volume.

A common method of constructing models of porous media is to place solid obstacles in a two- or three-dimensional test volume [15]. The properties of the medium are determined by the shape, size, and number of the obstacles, and by the distribution of the obstacles within the volume. In such ''materials'' with high porosity, all of the void space usually contributes to the flow through it. The effective porosity of the medium is then equal to the porosity. In contrast to this, for low porosity materials, a large part of the total void space may be nonconducting. For such media the effective porosity may therefore be significantly smaller than the geometrical porosity. At the percolation threshold, defined as the point where the medium becomes completely blocked, permeability and effective porosity both vanish. It is therefore clear that for porous media for which the percolation threshold appears at a finite porosity ϕ_c, the Kozeny equation, as given by Eqs. (2) or (3), is not valid for $\phi\to\phi_c$.

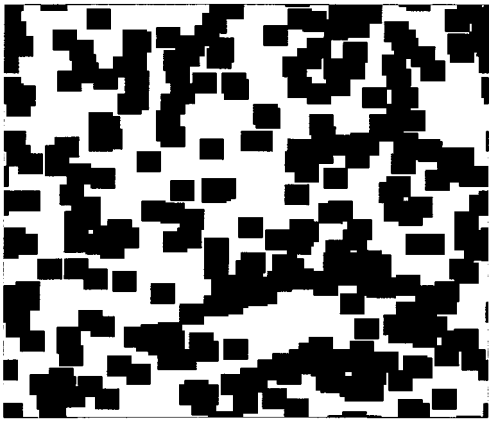

FIG. 1. A porous sample composed of 300 rectangles and having a porosity of $\phi=0.47$, and a dimensionless specific surface area of $S=0.69$.

The simplest way to modify Eqs. (2) and (3) to include the effect of nonconducting pores is to replace the porosity ϕ with the effective porosity $\phi_{\rm eff}$ (notice that in simple capillary models $\phi_{\rm eff}=\phi$). We thus obtain

$$k=\frac{\phi_{\rm eff}^3}{cS^2} \tag{4}$$

or

$$k=\frac{\phi_{\rm eff}^3}{c\tau^2S^2}. \tag{5}$$

At this point, we shall not try to substantiate Eqs. (4) and (5) further. Instead, we shall apply the lattice-gas cellular automaton method for fluid flow in a two-dimensional random porous medium, and compare the simulated results with permeabilities given by Eqs. (2), (3), (4), and (5). Notice that all three quantities $\phi_{\rm eff}$, τ, and S are functions of porosity.

In what follows we shall consider a simple model of porous media in which rectangles of equal size and unrestricted overlap are placed randomly in a two-dimensional volume (see Fig. 1). Although such a model may be considered somewhat artificial, it nevertheless captures much of the geometrical complexity of natural porous media, and gives a good testing ground for the validity of various permeability equations in two dimensions.

In order to compare various models of permeability with results of numerical simulations effectively, it is beneficial first to express the formulas Eqs. (2), (3), (4), and (5) as explicit functions of porosity ϕ alone. To do this, we have to find the dependence on the porosity ϕ of the specific surface area S, tortuosity τ, and effective porosity $\phi_{\rm eff}$.

For the model of freely penetrable obstacles, an analytical relation between the specific surface area and porosity can easily be found. Consider K freely overlapping obstacles of arbitrary but equal shape and size, and placed in a volume V in an n dimensional space. Let V_0 and A_0 be the volume and surface area of these obstacles, respectively. The expectation

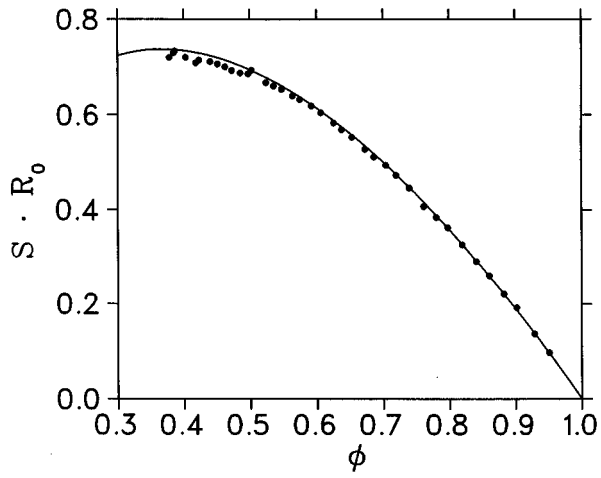

FIG. 2. The simulated dimensionless specific surface area SR_0 as a function of porosity ϕ. Here $R_0=18.6$ is the hydraulic radius of the rectangles. The statistical errors of the simulated values are smaller than the plotting symbols. The solid line is given by the theoretical expression Eq. (9) with $n=2$ (two-dimensional space).

value of the porosity ϕ is equal to the probability that a given point inside V is not overlapped by any of the K obstacles, i.e.,

$$\phi=\left(1-\frac{V_0}{V}\right)^K. \tag{6}$$

Similarly, the expectation value of the total surface area of the ensemble of obstacles, A, is given by the total number of obstacles times the surface area of a single obstacle times the probability that a given point on the surface of an obstacle is not overlapped by any other obstacle, i.e.,

$$A=KA_0\left(1-\frac{V_0}{V}\right)^{K-1}. \tag{7}$$

Solving the ratio V_0/V from Eq. (6), and using Eq. (7), we find that the specific surface area $S\equiv A/V$ is given by

$$S=\frac{n}{R_0}\phi^{(K-1)/K}\frac{1-\phi^{1/K}}{\frac{1}{K}}, \tag{8}$$

where $R_0=nV_0/A_0$ is the hydraulic radius of the obstacles. In the limits $K\to\infty$ and $V\to\infty$, such that the porosity ϕ remains constant, we obtain S in a simple and appealing form,

$$S=-\frac{n}{R_0}\phi\ln\phi \tag{9}$$

(see Fig. 2).

In an earlier work [35] we found numerically an approximate correlation $\tau=0.8(1-\phi)+1$ for the tortuosity in the case of freely penetrating rectangles. The simulations were then made for porosities greater than 0.5. In Sec. IV below we shall show new results reaching to $\phi=0.4$ [see Eq. (10) below]. We shall also present a corresponding approximative relation between the effective porosity and porosity [see Eq. (11) below].

III. LATTICE-GAS SIMULATIONS

We solved numerically the behavior of the two-dimensional creeping flow for the present model of random porous medium using the FHP-III lattice-gas method [17]. The number of fluid particles per lattice site was 3.5, which provides the best approximation for the solution of the linearized Navier-Stokes equation (creeping flow) within the present method [17]. With this density the logarithmic increase of viscosity with an increasing system size is also avoided [36]. Contrary to the common practice of imitating the permeability measurements, where the sample is placed in a tube [26,29,30], we imposed periodic boundary conditions on the lattice in both directions. This approach has the advantage of decreasing the finite-size effects, and, e.g., the boundary effects caused by fluid penetrating into the porous medium are eliminated. The fluid was forced to move in the positive x direction by applying an external force on the particles [36]. The porosity ϕ of the medium was defined as the ratio of the number of unoccupied sites to the number of all lattice sites.

The tortuosity and the effective porosity ϕ_{eff} were calculated using both 100×100 and 200×200 lattices with rectangles of 10×10 lattice sites. The larger lattice was used in the porosity region $\phi<0.55$. The number of different configurations was about 7 for the smaller lattice and 30 for the larger lattice. In these calculations, the velocity field was first allowed to saturate for 40 000 time steps for each configuration. The local velocities of the particles were then averaged over 400 000 time steps in order to ensure an undisturbed and smooth velocity field. The flow lines starting from each lattice site in the void space were found by interpolating the time-averaged flow velocity field. The tortuosity τ of each sample was then calculated using the method described in Ref. [35]. If the flow lines did not find their way through the whole medium, their starting points were assumed to lay in the nonconducting pore space. Finally, the effective porosity of each porous sample was calculated as the ratio of the number of those lattice sites from which the interpolation of the flow lines through the whole medium was successful, to the total number of lattice sites.

The specific surface area S and the permeability k were calculated using a 800×800 lattice with rectangles of 40×40 lattice sites. The number of rectangles K varied from 20 to 390 corresponding to porosities ranging from 0.95 to 0.38. The number of different configurations used at each K was ten in most cases. The number of iterations needed for reaching an adequate degree of saturation of the velocity field increased with an increasing porosity. The saturation time used in permeability calculations varied between 30 000 and 200 000 time steps. After saturation, the fluid velocity was found by averaging the particle velocities over 20 000 time steps.

In order to study the difference between random systems and regular lattices, which are often used in theoretical studies, we also made permeability simulations for systems in which the rectangles were placed in a regular square lattice.

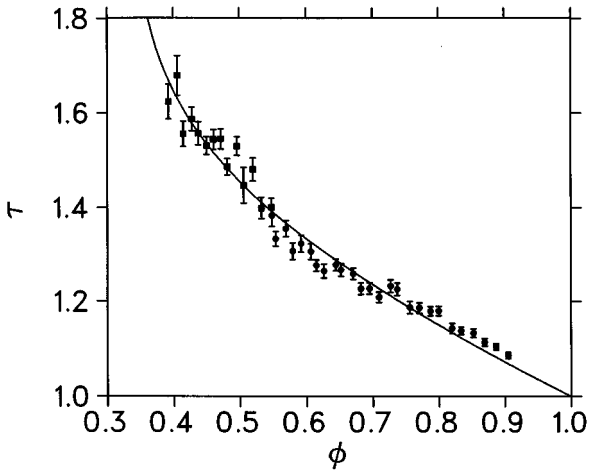

FIG. 3. The simulated tortuosity τ as a function of porosity ϕ. The solid squares show the values of tortuosity simulated for a 200 $\times$200 lattice, and the solid circles show the results from Ref. [35], where a 100$\times$100 lattice was used. The error bars include the statistical errors in tortuosity only. The solid line is the fit to the simulated points by Eq. (10).

In this case the number of rectangles varied from 16 to 256, which corresponded to porosities ranging from 0.96 to 0.36.

IV. RESULTS

In Fig. 1 we show an example of a porous medium constructed of 300 rectangles of size 40$\times$40 sites placed randomly in a 800$\times$800 lattice. The porosity of this sample was $\phi=0.47$ and the dimensionless specific surface area was $S=0.69$.

In Fig. 2 we show the plot of the simulated specific surface area S as a function of porosity ϕ together with the theoretical curve, Eq. (9). The values of S are expressed here in dimensionless form, being multiplied by the hydraulic radius R_0 of the rectangles. Notice that due to the triangular simulation lattice used here, the vertical sides of the rectangles are shorter than the horizontal sides by a factor of $\sin(\pi/3)$. The hydrodynamic radius was therefore $R_0\approx 18.6$ lattice spacings.

The simulated values of tortuosity τ are shown in Fig. 3 as a function of porosity ϕ. Also shown in this figure is a fit to the simulated values using a function of the form

$$\tau=1+a\frac{(1-\phi)}{(\phi-\phi_c)^m}, \tag{10}$$

with the values of the fitting parameters being $a=0.65$ and $m=0.19$. The expression Eq. (10) has been chosen such that tortuosity is a monotonously decreasing function of porosity (at $\phi>\phi_c$) and diverges at the percolation threshold ϕ_c [15]. For the present system the percolation threshold is $\phi_c=0.33$ [37].

The conducting pore space (white regions) of the porous sample shown in Fig. 1, and determined by the method described above, is shown in Fig. 4. The (geometrical) porosity of the sample is $\phi=0.47$ while the effective porosity in this particular case is $\phi_{\rm eff}=0.40$.

In Fig. 5 we show the simulated values of the effective

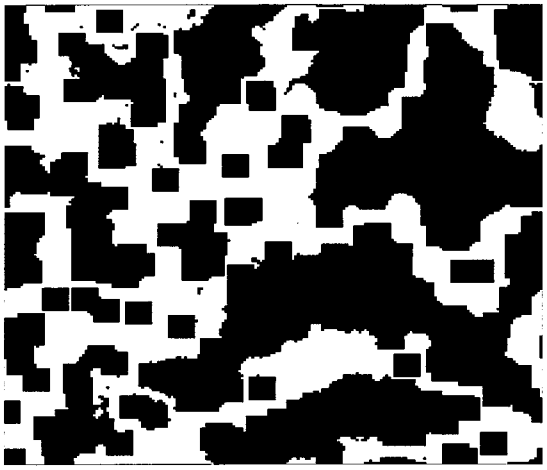

FIG. 4. The conducting pore space of the porous sample shown in Fig. 1 corresponding to an effective porosity $\phi_{\rm eff}=0.40$.

porosity as a function of porosity. The error bars shown include only the statistical error associated with the random positioning of the obstacles. The solid line shown in Fig. 5 is a fit to the calculated points by

$$\phi_{\rm eff}=ax^3-(2a+\phi_c)x^2+(a+1+\phi_c)x, \tag{11}$$

where $x=(\phi-\phi_c)/(1-\phi_c)$. The fitted value of the parameter a is $a=0.3$. The expression Eq. (11) is simply the most general third-order polynomial in which the natural constraints, $\phi_{\rm eff}=d\phi_{\rm eff}/d\phi=1$ at $\phi=1$, and $\phi_{\rm eff}=0$ at $\phi=\phi_c=0.33$, have been implemented. With the given values of ϕ_c and a, this expression also fulfills the condition that $\phi_{\rm eff}\leqslant\phi$ for all $\phi\leqslant 1$. We emphasize that the true functional form of $\phi_{\rm eff}$ as a function of ϕ is not known. Expressions other than Eq. (11) can also be found which would give a good quantitative fit to the results of the present simulation. As an example we give the expression $\phi_{\rm eff}=1-\ln\phi/\ln\phi_c$, which gives a good quantitative fit to the simulated results, but, with porosities higher than 0.8, the expression produces

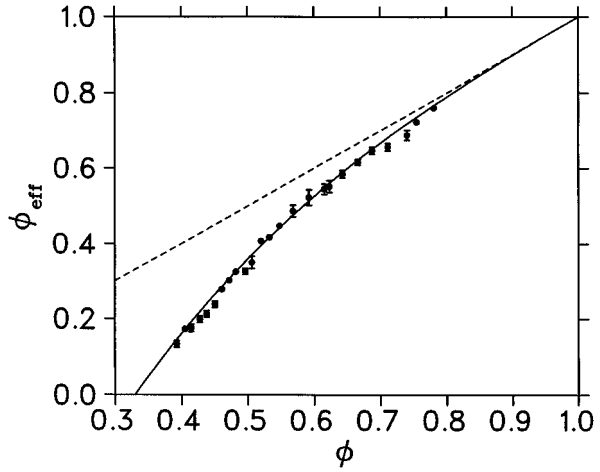

FIG. 5. The simulated effective porosity $\phi_{\rm eff}$ as a function of porosity ϕ. The solid line is the fit by Eq. (11), and the dotted line is the curve $\phi_{\rm eff}=\phi$. The error bars include only the statistical errors in the effective porosity.

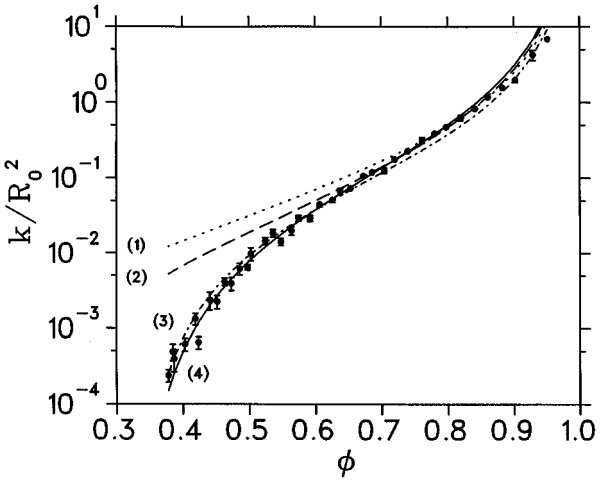

FIG. 6. The simulated dimensionless permeability k/R_0^2 of the porous system as a function of porosity ϕ. The error bars show the statistical errors in permeability. Curves 1–4 show the predictions given by the permeability expressions Eqs. (2)–(5), respectively.

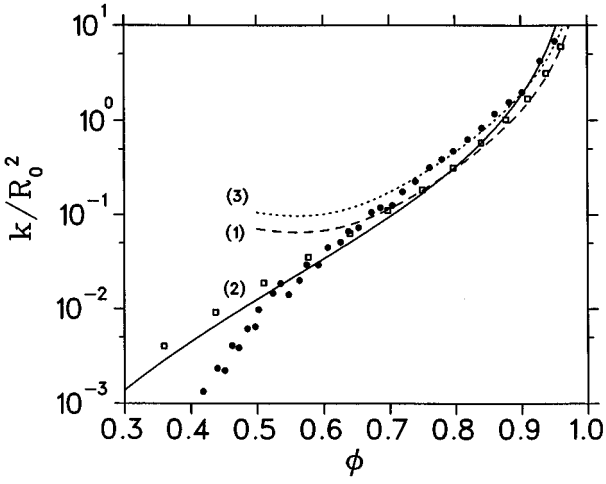

FIG. 7. The simulated dimensionless permeabilities k/R_0^2 of the random porous system (solid circles) and the regular lattice (open squares) as a function of porosity. Curve 1 shows the permeability given by the unit cell approach, Eq. (12). Curve 2 shows the permeability given by the Kozeny law, Eq. (2). Curve 3 shows the permeability of Eq. (12) multiplied by 1.5.

ϕ_{eff} larger, if only very slightly, than ϕ. It thus fails to give a qualitatively correct behavior in this porosity region.

The permeabilities simulated for the model system are shown in Fig. 6. The error bars again include the statistical errors in permeability only. Also shown are the predictions given by the permeability expressions, Eqs. (2)–(5), with S, τ, and ϕ_{eff} given by Eqs. (9), (10), and (11), respectively, with the theoretical value $\phi_c = 0.33$. Here the Kozeny coefficient c was used as the fitting parameter. The permeabilities were made dimensionless by dividing by the hydraulic radius R_0 squared. For expressions Eqs. (2) and (3) (curves 1 and 2 in Fig. 6), fits to all of the data points were clearly unsatisfactory. Therefore fits were made, instead, in a narrow porosity region at midporosities, where these formulas seem to give a qualitatively correct porosity dependence for the simulated permeabilities. For expressions (4) and (5) (curves 3 and 4 in Fig. 6), fits were made to all data points.

As can be seen from Fig. 6, the porosity region in which the Kozeny equation in its basic form, Eq. (2), is adequate for this particular system, is quite narrow. Taking into account the effect of tortuosity by Eq. (3) improves the fit only slightly. The result is significantly improved only by introducing the effective porosity, Eq. (4), and an even better result is obtained by Eq. (5) in which the tortuosity and effective porosity are both included.

The fitted values of the Kozeny coefficient c were 8.2, 6.5, 10.4, and 5.8 for Eqs. (2), (3), (4), and (5), respectively. This is in good agreement with various models and measurements found in literature, where values for the Kozeny coefficient c typically reported are in the range from 2 to 12 [1,2,4].

A three-dimensional simulation of fluid flow through a bed of penetrable spheres was made earlier in Ref. [25], where good quantitative agreement with the Kozeny equation (2) was obtained down to $\phi \approx 0.1$, below which there was still a good qualitative fit. The difference between these and the present results is caused by the weaker tendency in that case to form dead-end pores, and the much lower value of the percolation threshold ϕ_c of the three-dimensional system used in Ref. [25] in comparison with the two-dimensional system used here. Therefore, for such a three-dimensional system, effective porosity may be close to the geometrical porosity also for rather low values of the porosity.

The permeabilities simulated for the regularly arranged rectangles are shown in Fig. 7 with open squares. The curve number 1 shows the prediction for the permeability of this system as given by the unit cell approach [5], namely

$$k = \frac{R_0^2}{8\epsilon}[-\ln\epsilon - 1.476 + 2\epsilon - 1.774\epsilon^2 + 4.076\epsilon^3 + O(\epsilon^4)], \tag{12}$$

where $\epsilon = 1 - \phi$. It is evident from Fig. 7 that the expression Eq. (12) approximates the simulated permeabilities with a reasonably good accuracy for porosities higher than 0.6. For lower porosities the unit cell approach seems to fail. Curve number 2 in Fig. 7 shows the permeability as given by Eq. (2). Here the fit was made for all data points with the result $c = 9.9$. Contrary to random systems, the Kozeny equation seems to give a reasonably good approximation for the permeability of a regular square lattice.

Theoretical analyses and measurements both suggest that, for inhomogeneous systems in which the obstacles are placed randomly without overlapping, inhomogeneity can increase the permeability by as much as 50% as compared to a regular lattice [5]. This result also holds for systems with overlapping obstacles and high porosities when the probability of overlapping is small. Curve number 3 in Fig. 7 shows the prediction of the unit-cell approach Eq. (12) with a 50% increase added to it. This curve is seen to approximate the simulated permeabilities for the random system only for porosities higher than 0.7.

Near the percolation threshold $\phi = \phi_c$, the permeability of a porous medium often follows a scaling law of the form

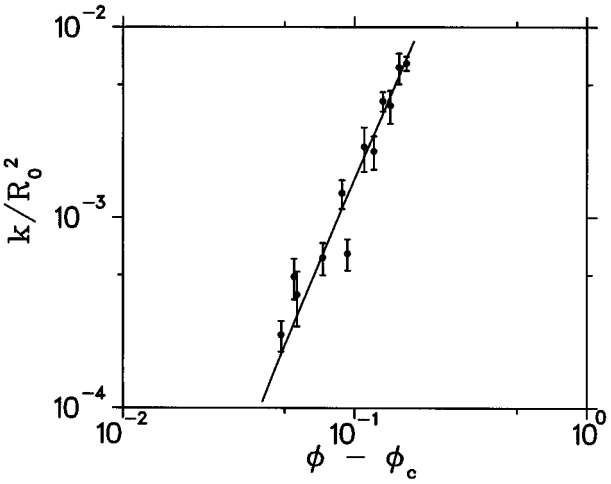

FIG. 8. The simulated dimensionless permeability k/R_0^2 of the random porous system as a function of $\phi-\phi_c$. The solid line is the fit by Eq. (13) with $a=350$, $\phi_c=0.33$, and $\mu=2.8$.

$$k=a(\phi-\phi_c)^{\mu}. \tag{13}$$

A three-parameter fit by the scaling law Eq. (13) to the simulated permebilities in the region $\phi<0.5$, shown in Fig. 8, gives the critical exponent $\mu=2.8$, the percolation threshold $\phi_c=0.33$, and the constant of proportionality $a=350$. Notice that the value of the critical exponent μ obtained here is equal to that obtained for a model in which circles are used instead of rectangles [15].

V. ERROR ESTIMATES

The accuracy of lattice-gas simulations depends on the ratios of the mean free path λ of the fluid particles to the sizes of the obstacles and pores [22–24,29,30]. The simulated flow field does not approach the continuum limit unless these ratios are small. The finite size dependence of permeability is known [29] to obey the scaling law $k\propto 1+\alpha/R$, where R is the characteristic size of the system in lattice units, and α is a constant that depends on the details of the simulation model used. We studied the finite lattice size effects for a varying porosity using $L\times L$ lattices with L varying in the range $100\leqslant L\leqslant 800$. The size of the rectangles used in these simulations was $L/20$ or $L/10$. With porosities higher than 0.5, the average relative error of the calculated permeabilities due to the finite lattice size (800×800) was estimated to be less than 5% .

Due to the finite-size effects, simulations by the present method of fluid flow in a random medium with low porosity, will not produce accurate results when the porosity ϕ is very close to the percolation threshold [23,29]. The error in permeability due to finite-size effects was estimated to be less than 10% for $\phi=0.40$. Therefore, the simulations appear to be quite accurate in the whole porosity region analyzed here. This conclusion is also substantiated by the reasonable value found for the critical exponent μ of permeability close to the percolation threshold.

VI. DISCUSSION

We used the lattice-gas method to simulate numerically a creeping flow of Newtonian fluid through a two-dimensional porous substance that is composed of randomly placed rectangles of equal size and unrestricted overlap. Numerical correlations were found between the specific surface, tortuosity, effective porosity, permeability, and porosity of the model porous structure. It was an important part of the analysis that the dependence on porosity of the specific surface area was also derived analytically for the medium. In fact the analytical result is applicable to a slightly more general case in which the medium consists of particles of arbitrary but equal shape.

Effective porosity, as well as tortuosity, were determined by simulations as functions of porosity. Excellent polynomial fits were found to the simulated points, but it was not possible to deduce simple analytical expressions for these quantities that would have been qualitatively correct in the whole porosity range.

Several modifications of the Kozeny law for permeability were compared with the numerical results found by the lattice-gas simulations. The original Kozeny equation was found to hold within a narrow porosity region $0.7<\phi<0.9$ only. The discrepancy observed at lower values of porosity was found to arise from the tendency in that case of the model porous medium to form small nonconducting pores. Excellent agreement was found between the numerical results and a modified Kozeny law, Eq. (5), in which the effects of both the tortuosity and effective porosity were taken into account. The inclusion of the effective porosity in the expression for permeability was found to play the major role in this agreement, being of crucial importance for porosities approaching the percolation threshold $\phi=\phi_c$.

It was possible to simulate the permeability even quite close to the percolation threshold. A clear scaling behavior extending over two orders of magnitude was found for k. The scaling exponent $\mu=2.8$ found in this way agrees well with that derived previously for a similar model porous medium composed of two-dimensional spheres. Simulations of effective porosity and tortuosity could not be reliably made close enough to the percolation threshold, such that the scaling behavior in this limit of these quantities could have been found.

Permeability of a regular array of rectangles was also simulated. Very much as expected, for $\phi>0.7$ the permeability of the regular lattice is lower than that of randomly positioned rectangles with the same porosity, the latter being 1.5 times bigger. For low porosities, $\phi<0.55$, the permeability of the regular lattice is of course higher as there is no percolation threshold in this case.

It is evident that the permeability of two-dimensional random porous media is very much affected by restrictions on flow caused by narrow passages and dead-end pores. There is some previous evidence that these effects are not nearly so important in three dimensions. It may well be, however, that the actual structure of the pore space available for flow plays an important role in three dimensions. It remains to be seen, e.g., if effective porosity becomes important for such three-dimensional porous structures in which the percolation threshold is relatively high.

[1] A. E. Scheidegger, *The Physics of Flow Through Porous Media* (MacMillan, New York, 1957).
[2] J. Bear, *Dynamics of Fluids in Porous Media* (Dover, New York, 1972).
[3] M. Sahimi, Rev. Mod. Phys. **65**, 1393 (1993).
[4] S. T. Han, Pulp Paper Mag. Can.**70**, T134 (1969).
[5] G. W. Jackson and D. F. James, Can. J. Chem. Eng. **64**, 364 (1986).
[6] K.-H. Hellmuth, P. Klobes, K. Meyer, B. Röhl-Kuhn, M. Siitari-Kauppi, J. Hartikainen, K. Hartikainen, and J. Timonen, Z. Geol. Wiss. **23**, 691 (1995).
[7] D. L. Johnson, J. Koplik, and L. M. Schwartz, Phys. Rev. Lett. **57**, 2564 (1986).
[8] S. Kostek, L. M. Schwartz, and D. L. Johnson, Phys. Rev. B **45**, 186 (1992).
[9] A. J. Katz and A. H. Thompson, J. Geophys. Res. B **92**, 599 (1987).
[10] D. J. Wilkinson, D. L. Johnson, and L. M. Schwartz, Phys. Rev. B **44**, 4960 (1991).
[11] A. H. Thompson, S. W. Sinton, S. L. Huff, A. J. Katz, R. A. Raschke, and G. A. Gist, J. Appl. Phys. **65**, 3259 (1989).
[12] D. L. Johnson, D. L. Hemmick, and H. Kojima, J. Appl. Phys. **76**, 104 (1994).
[13] F. A. L. Dullien, *Porous Media. Fluid Transport and Pore Structure* (Academic, San Diego, 1979).
[14] Yu. A. Buyevich, Int. J. Heat Mass Transf. **35**, 2445 (1992).
[15] M. Sahimi, *Flow and Transport in Porous Media and Fractured Rock* (VCH, Weinheim, 1995).
[16] A. J. Katz and A. H. Thompson, Phys. Rev. B **34**, 8179 (1986).
[17] U. Frisch, D. d'Humiéres, B. Hasslacher, P. Lallemand, Y. Pomeau, and J.-P. Rivet, Complex Syst. **1**, 649 (1987).
[18] D. H. Rothman and S. Zaleski, Rev. Mod. Phys. **66**, 1417 (1994).
[19] G. R. McNamara and G. Zanetti, Phys. Rev. Lett. **61**, 2332 (1988).
[20] Y. H. Qian, D. d'Humiéres, and P. Lallemand, Europhys. Lett. **17**, 479 (1992).
[21] R. Benzi, S. Succi, and M. Vergassola Phys. Rep. **222**, 145 (1992).
[22] I. Ginzbourg and D. d'Humierés, J. Stat. Phys. **84**, 927 (1996).
[23] D. H. Rothman and S. Zaleski, *Lattice Gas Cellular Automata* (Cambridge University Press, Cambridge, 1997).
[24] D. H. Rothman, Geophysics **53**, 509 (1988).
[25] A. Cancelliere, C. Chang, E. Foti, D. H. Rothman, and S. Succi, Phys. Fluids A **2**, 2085 (1990).
[26] M. Sahimi and D. Stauffer, Chem. Eng. Sci. **46**, 2225 (1991).
[27] S. Chen, K. Diemer, G. D. Doolen, K. Eggert, C. Fu, S. Gutman, and B. J. Travis, Physica D **47**, 72 (1991).
[28] U. Brosa and D. Stauffer, J. Stat. Phys. **63**, 405 (1991).
[29] G. A. Kohring, Physica A **186**, 97 (1992).
[30] J. F. McCarthy, Phys. Fluids **6**, 435 (1994).
[31] S. Succi, E. Foti, and F. Higuera, Europhys. Lett. **10**, 433 (1989).
[32] A. K. Gunstensen and D. H. Rothman, J. Geol. Res. **98**, 6431 (1993).
[33] A. J. C. Ladd, J. Fluid Mech. **271**, 285 (1994).
[34] A. J. C. Ladd, J. Fluid Mech. **271**, 311 (1994).
[35] A. Koponen, M. Kataja, and J. Timonen, Phys. Rev. E **54**, 406 (1996).
[36] L. P. Kadanoff, G. R. McNamara, and G. Zanetti, Phys. Rev. A **40**, 4527 (1989).
[37] G. E. Pike and C. H. Seager, Phys. Rev. B **10**, 1421 (1974).